

Optimal Shape of Fibers in Transmission Problem

P.P. Prochazka¹ and M.J. Valek¹

Abstract: In classical theories of homogenization and localization of composites the effect of shape of inclusions is not taken into account. This is probably done because of very small fibers in classical composites based on epoxy matrix. Applying more precise theoretical and numerical tools appears that the classical theories desire corrections in this direction. Today many types of materials their fiber are much bigger and with various material properties are used and behave as typical composites. They enable producers to create the fiber cross-sections and model them in various shapes, so that it is meaningful to carry out the optimization. In the paper optimal shape of fibers is sought to admit as small amount of heat energy to pass through a composite as the constituents allow.

Keywords: Shape optimization, composites, heat transfer, minimum energy.

1 Introduction

In the paper optimal shape of fibers is identified in a symmetric unit cell, which is positioned in a composite structure. Harmonic problem is to be solved with a typical application to linear conductivity or transmission problem. The coefficients of conductivity are given in advance as uniformly distributed in the phases with different values in the fiber and the matrix. Hence, the design parameters are linked by the shape of fiber, which is assumed as star-shaped to be in compliance with a reasonable formulation of the problem. Since a moving boundary problem is basically discussed, boundary element method appears to be the most appropriate in this application. Since the problem desires a constraint in order to be unisolvent, necessary conditions have to be imposed. First, a reasonable condition is the choice of the volume (in 2D the area) of fiber. On the other hand it appears that in certain cases of the fiber volume fraction (the given area) still the problem can lead to a nonrealistic result. This is why additional constraints have to be added. This occurs as the prescribed measure of the fiber is calculated in an integral form, i.e. positive and negative signs of areas may cause a nonrealistic geometry. For that, limits on

¹ CTU in Prague, Czech Republic.

the shape characteristics should be added, such as the diameters or tangential slope of certain directions of the interfacial fiber-matrix boundary. Then the mathematical formulation and subsequent numerical treatment provide a reasonable, fully usable in practice, layouts.

Optimization of coupled elasticity and conductivity problem is solved in Challis et al (2008) for maximized stiffness and conductivity. Hereinafter similar procedure as that used in Prochazka et al (2009) is applied for formulating and calculating the proper shape of fibers.

Classical approach in localization and homogenization of elastic composites belongs to Suquet (1985), and that of steady state heat transfer can be found in Lévy (1985). In both latter publications a periodic structure of composites is preferred from other possible boundary conditions along the unit cell. The meaning “periodic structure” is explained for periodic representative element. Such a procedure is applied in this paper to unit cell concept. The optimization of the shape of fiber in a composite structure due to a heat load is discussed in Dvorak (1996), where the problem of a variance between given overall properties and that calculated from the given material properties of phases is as small as possible. Fiber shape optimization in linear elasticity is presented in Prochazka (2012a) based on boundary element method. A comprehensive review of optimization methods in structures is brought forward in Akad et al (2012) with large extent of references on the topic. In Prochazka (2012b) a special material is optimized namely a composite with a hole. The hole has various volume ratios and the shapes of the hole are compared and their impact evaluated. Paper Zhoua and Lia (2008) is concern with the similar problem as that studied in this work, but the methodology differs. Finally, Allaire issued a book on optimization based on homogenization, which covers both the topological and moving boundary approaches and serve till today as one of establishing theories of optimization using homogenization.

In this text the steady state problem is studied. It involves heat and mass density transfer, filtration of the Newtonian liquid, etc. First, homogenization technique will be suggested and a variational formulation will characterize the optimization problem, so that the formulation in terms of boundary elements can easily be derived. The selected cost functional will provide designers with a range of possible conditions according to their request.

2 Basic considerations and equations

In this paper transmission or steady state heat transfer in composite structure is to be treated. Unidirectional parallel filaments perpendicular to the cross-section of the composite are assumed, i.e. two-dimensional problem is presumed. In the cross-

section two-phase composite is taken into account with one phase denoted as fiber and the other as matrix, both positioned in a periodic unit cell, which is cut out of a representative volume element V (denoted as RVE) describing the neighborhood of a typical point of a macrostructure.

Let the domain representing the composite body is denoted as $\Omega \subset V \in \mathbb{R}^2$ and its boundary $\partial\Omega$ is supposed to be Lipschitz continuous. Isotropic phases $\Omega_f \subset \Omega$ and $\Omega_m \subset \Omega$ represent the fiber and the matrix, respectively. The boundary of the fiber (i.e. the interfacial boundary Γ_C) is in any case bounding the fiber in such a way that it is star shaped, i.e. there is a point (pole, in our case the center of the unit cell) and to each point inside of the fiber there is an abscissa connecting the pole and the current point which is completely imbedded in the fiber. Fig. 1 offers a layout used in what follows. Note that more general shapes are mentioned in Dvorak (1996), where a special treatment on how to simplify complicated unit cells is also discussed based on body transformations creating a group of base bodies.

In RVE coordinate system $0x_1x_2$ is introduced while the unit cells are equipped by local coordinate system $0y_1y_2$, since 2D problem is discussed.

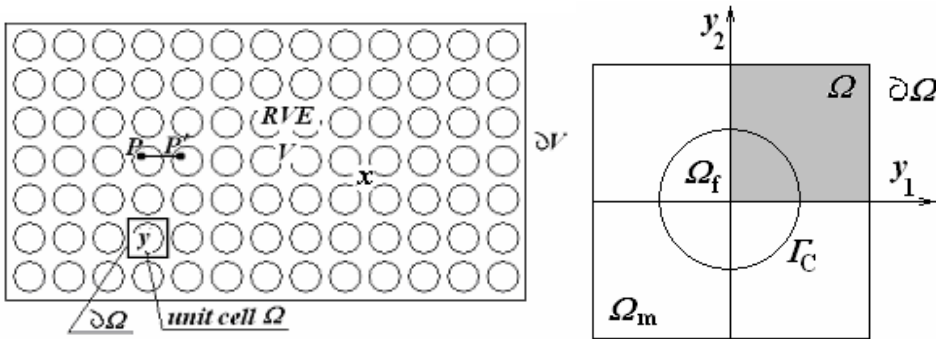


Figure 1: Geometries of RVE and unit cell

Now the periodic conditions will be précised. The unit cells in the RVE are homothetic, i.e. there is a constant, say ℓ , and to any point $P \in V$ is always P' , which is identified by the law: $P'(x) = P(x + \ell) = \ell P P'$, and the function to be considered as periodic has exactly the same value at and P' . In our case a square unit cell is taken into account. Hence the homothetic property is applicable in both x_1 and x_2 directions. Denote the macroscopic length of RVE. The periodicity can also be defined in the following way: take a small number $\varepsilon = \ell/L$, and consequently, $\Omega = \varepsilon V$.

The conservation law is assumed in the standard divergence form applied to tem-

perature $u^\varepsilon(x)$ for arbitrary ε as,

$$\frac{\partial}{\partial x_i}(c^\varepsilon(x))\frac{\partial}{\partial x_i}u^\varepsilon(x) = 0, \quad i = 1, 2 \tag{1}$$

where $c^\varepsilon \equiv c^\varepsilon(x) = c(x/\varepsilon) = c(y)$ is dependent on the position in Ω . The fiber Ω_f , and matrix Ω_m are equipped with generally different conductivities c_f (fiber) and c_m (matrix), where c_f and c_m are uniformly distributed inside of the appropriate phases. This means that the coefficient of conductivity $c(y)$ is defined as:

$$c(y) = c_f \text{ for } y \in \Omega_f \text{ and } c(y) = c_m \text{ otherwise} \tag{2}$$

The partial equations are written as

$$\nabla q^\varepsilon(x) = 0, \quad q^\varepsilon(x) = c^\varepsilon(x)\nabla u^\varepsilon(x) \tag{3}$$

where ∇ is the nabla operator with respect to x , and q^ε is the flux vector, gradient of weighted u^ε .

For statistically isotropic material with the periodic boundary conditions an analog of the well known Hill's condition in elasticity holds valid as:

$$\begin{aligned} \langle q^\varepsilon \nabla u^\varepsilon \rangle &= \frac{1}{\text{meas } \Omega} \int_{\Omega} q^\varepsilon \nabla u^\varepsilon \, d\Omega(y) = \langle q^\varepsilon \rangle \langle \nabla u^\varepsilon \rangle = \\ &= \frac{1}{\text{meas } \Omega} \int_{\Omega} q^\varepsilon \, d\Omega(y) \times \frac{1}{\text{meas } \Omega} \int_{\Omega} \nabla u^\varepsilon \, d\Omega(y) \end{aligned} \tag{4}$$

where $\text{meas } \Omega$ is the volume in 3D or area in 2D, mostly considered equal to unit.

3 Homogenization

In order to get relations between local and overall properties of the composite an asymptotic expansion of u^ε and q^ε are considered for each ε :

$$\begin{aligned} u^\varepsilon(x) &= u^0(x, y) + \varepsilon u^1(x, y) + \dots \\ q^\varepsilon(x) &= q^0(x, y) + \varepsilon q^1(x, y) + \dots \end{aligned} \quad y = x/\varepsilon, \tag{5}$$

where u^i and q^i are Ω -periodic in x . In what follows coordinates x and y are first taken as independent and afterwards y is substituted by x/ε . If the differentiation of the first order is applied to Eq. (1), the operator $\frac{\partial}{\partial x_i}$ is read as $\frac{\partial}{\partial x_i} + \frac{1}{\varepsilon} \frac{\partial}{\partial y_i}$. Substituting Eq. (5) to Eq. (1) and considering the previous replacement in differentiation yields:

$$\left(\frac{\partial}{\partial x_i} + \frac{1}{\varepsilon} \frac{\partial}{\partial y_i} \right) \left[c^\varepsilon \left(\frac{\partial}{\partial x_i} + \frac{1}{\varepsilon} \frac{\partial}{\partial y_i} \right) u^\varepsilon \right] = 0 \tag{6}$$

and doing the latter binomials and product leaves:

$$\left[\frac{\partial}{\partial x_i} \left(c^\varepsilon \frac{\partial}{\partial x_i} \right) + \frac{1}{\varepsilon} \frac{\partial}{\partial y_i} \left(c^\varepsilon \frac{\partial}{\partial x_i} \right) + \frac{1}{\varepsilon} \frac{\partial}{\partial x_i} \left(c^\varepsilon \frac{\partial}{\partial y_i} \right) + \frac{1}{\varepsilon^2} \frac{\partial}{\partial y_i} \left(c^\varepsilon \frac{\partial}{\partial y_i} \right) \right] \times (u^0(x, y) + \varepsilon u^1(x, y) + \dots) = 0 \quad (7)$$

which at $O(\varepsilon^{-2})$ produces the condition:

$$\frac{\partial}{\partial y_i} \left(c \frac{\partial}{\partial y_i} u^0 \right) = 0 \Rightarrow u^0(x, y) = u^0(x) \quad (8)$$

where $c^\varepsilon \equiv c^\varepsilon(x) = c(x/\varepsilon) = c(y)$ is dependent on the position in Ω and $u^0(x)$ is independent of y , i.e. it is a parameter to be stated later on. From Eq. (5) at $O(\varepsilon^{-1})$ one gets:

$$q_i^0(x, y) = c(y) \left(\frac{\partial u^0}{\partial x_i} + \frac{\partial u^1}{\partial y_i} \right), \quad \dots \quad (9)$$

and Eq. (7) becomes:

$$\frac{\partial}{\partial y_i} \left[c(y) \left(\frac{\partial u^1}{\partial y_i} + \frac{\partial u^0}{\partial x_i} \right) \right] = 0 \quad (10)$$

in the sense of distributions. In order to avoid the term $\frac{\partial u^0}{\partial x_i}$ for the differential equation (10) to be written only in y_i a substitution is introduced:

$$u^1 = \frac{\partial u^0}{\partial x_k} w_k(y) + \tilde{u}^1(x) \Rightarrow \frac{\partial}{\partial y_i} \left[c(y) \frac{\partial w_k}{\partial y_i} \right] = - \frac{\partial}{\partial y_i} [c(y) \delta_{ik}] \quad (11)$$

Eq. (11) is the starting equation for solving u^1 depending on w_k known from the calculation approach. It appears that there is a unique solution u^1 of Eq. (10) for u^0 given but an additional term, which can be disregarded, Haslinger and Dvorak (1995), Lévy (1985) and the same property possesses w_k . This is an elliptic equation being defined in Ω . Closer look at (11) shows that the left hand side is regular and the right hand side is incorrect from the point of view of classical theory. Since similarly to elastic problem the Laplace equation (1) is linear, the approach to evaluation of the right hand side can be developed to decode the generalized terms. Multiply both sides by a smooth enough function ϕ , which is not identically equal to zero (test function) and integrate over Ω to get:

$$\int_{\Omega} \frac{\partial}{\partial y_i} \left[c(y) \frac{\partial w_k}{\partial y_i} \right] \phi \, d\Omega = - \int_{\Omega} \frac{\partial c(y)}{\partial y_k} \phi \, d\Omega \quad (12)$$

As mentioned previously the left hand side is “well-defined”, if u^1 and $w_k \in H^1(\Omega)$ and are Ω -periodic. The right hand side, on the contrary, has to be studied more attentively. Using the second Green’s theorem it successively holds:

$$\begin{aligned}
 - \int_{\Omega} \frac{\partial c(y)}{\partial y_k} \phi \, d\Omega &= - \int_{\partial\Omega_f} c(y) \phi \, n_k^f \, d(\partial\Omega_f) - \int_{\partial\Omega_m} c(y) \phi \, n_k^m \, d(\partial\Omega_m) + \\
 &+ c_f \int_{\Omega_f} \frac{\partial \phi}{\partial y_k} \, d\Omega_f + c_m \int_{\Omega_m} \frac{\partial \phi}{\partial y_k} \, d\Omega_m
 \end{aligned} \tag{13}$$

where $n^f = \{n_1^f, n_2^f\}$ is the outward unit normal to Ω_f and $n^m = \{n_1^m, n_2^m\}$ is the outward unit normal to Ω_m .

On the other hand $\partial\Omega_f = \Gamma_C$ and $\partial\Omega_m = \partial\Omega \cup \Gamma_C$, as seen in Fig. 1. Hence, Eq. (13) may be recorded as,

$$\begin{aligned}
 - \int_{\Omega} \frac{\partial c(y)}{\partial y_k} \phi \, d\Omega &= - \int_{\Gamma_C} c_f \phi \, n_k^f \, d\Gamma_C - \int_{\Gamma_C} c_m \phi \, n_k^m \, d\Gamma_C - \\
 &- \int_{\partial\Omega} c(y) \phi \, n_k \, d(\partial\Omega) + \int_{\Omega_f} c(y) \frac{\partial \phi}{\partial y_k} \, d\Omega_f + \int_{\Omega_m} c(y) \frac{\partial \phi}{\partial y_k} \, d\Omega_m
 \end{aligned} \tag{14}$$

It is worth noting that since obviously $n^f = -n^m$, the weak formulation leading to the application of finite element method can be restored as: find $u_1 \in H^1(\Omega)$, so that the following equations are fulfilled for each $\phi \in H^1(\Omega)$ (both functions obey the periodic boundary conditions):

$$\begin{aligned}
 - \int_{\Omega} c(y) \frac{\partial w_k}{\partial y_i} \frac{\partial \phi}{\partial y_i} \, d\Omega &= \\
 = - \int_{\Gamma_C} [c_f - c_m] \phi \, n_k^f \, d\Gamma_C - \int_{\partial\Omega} c(y) \phi \, d(\partial\Omega) + \int_{\Omega} c(y) \frac{\partial \phi}{\partial y_i} \, d\Omega_f
 \end{aligned} \tag{15}$$

Coming back to the classical formulation gives:

$$\frac{\partial}{\partial y_i} \left[c(y) \frac{\partial w_k}{\partial y_i} \right] = -q_C^k \delta_{\Gamma_C} \tag{16}$$

and the periodic boundary conditions, where q_C^k are interfacial flows and δ_{Γ_C} is the distributed Dirac’s function along the interface between the phases. The formula is in compliance with Suquet (1985), who submitted it for linear elasticity. From Eq. (14) it holds:

$$q_C^k(y) = [c_f - c_m] n_k^f(y) \tag{17}$$

Hereinafter an axisymmetric problem makes sense to be considered without loss of generality. Moreover, star-shaped fibers are supposed, i.e. there is a point (origin of the coordinate system) the rays from which cross the interfacial segment only and only once. For this reason the first quarter is considered in what follows, see Fig. 1, the shaded part.

4 Boundary element formulation

Since the shape optimization is closely related to a moving boundary problem the boundary element formulation seems to be extremely advantageous. Simple substructuring will be applied. Starting equation will be Eq. (16) with the right hand side equal to $-q_C^k \delta_{\Gamma_C}$ representing the distributed Dirac function, which is multiplied by a function u^* , integrated successively over Ω_f and Ω_m applying linear approximations over boundary elements and splitting the boundaries into that lying on Γ_C and the remaining parts finally yields:

$$\begin{aligned} c(\xi)u(\xi) &= \int_{\partial\Omega_f} q(y)u^*(y, \xi) d\Gamma(y) - \int_{\partial\Omega_f} u(y)q^*(y, \xi) d\Gamma(y) = \\ &= \int_{\partial\Omega_f - \Gamma_C} q(y)u^*(y, \xi) d\Gamma(y) - \int_{\partial\Omega_f - \Gamma_C} u(y)q^*(y, \xi) d\Gamma(y) + \\ &+ \int_{\Gamma_C} q(y)u^*(y, \xi) d\Gamma(y) + \int_{\Gamma_C} u(y)q^*(y, \xi) d\Gamma(y), \quad \xi \in \partial\Omega_f \end{aligned} \quad (18)$$

$$\begin{aligned} c(\xi)u(\xi) &= \int_{\partial\Omega_m} q(y)u^*(y, \xi) d\Gamma(y) - \int_{\partial\Omega_m} u(y)q^*(y, \xi) d\Gamma(y) = \\ &= \int_{\partial\Omega_m - \Gamma_C} q(y)u^*(y, \xi) d\Gamma(y) - \int_{\partial\Omega_m - \Gamma_C} u(y)q^*(y, \xi) d\Gamma(y) + \\ &+ \int_{\Gamma_C} q(y)u^*(y, \xi) d\Gamma(y) + \int_{\Gamma_C} u(y)q^*(y, \xi) d\Gamma(y), \quad \xi \in \partial\Omega_m \end{aligned} \quad (19)$$

where $u = w_k$ for simplicity, $u^* = \log \frac{1}{r(\xi, y)}$ is the fundamental solution, r is the Euclidean distance between points y and ξ , and $q^* = \frac{\partial u^*}{\partial n}$, n is again outward unit normal to the appropriate domain; c equals the internal angle of the boundary at ξ . Equations (18-19) enable us to use substructuring. Applying a linear spline interpolation in these equations yields:

$$\begin{bmatrix} K_{11}^f & K_{12}^f \\ K_{21}^f & K_{22}^f \end{bmatrix} \begin{Bmatrix} u_f^{\text{out}} \\ u_f^{\text{in}} \end{Bmatrix} = \begin{Bmatrix} q_f^{\text{out}} \\ q_f^{\text{in}} \end{Bmatrix}, \quad \begin{bmatrix} K_{11}^m & K_{12}^m \\ K_{21}^m & K_{22}^m \end{bmatrix} \begin{Bmatrix} u_m^{\text{in}} \\ u_m^{\text{out}} \end{Bmatrix} = \begin{Bmatrix} q_m^{\text{in}} \\ q_m^{\text{out}} \end{Bmatrix}, \quad (20)$$

$K_{ij} = B_{ik}^{-1} A_{kj}$ where $A_{ij} u_j = B_{ij} q_j$

where u and q are vectors of temperature w_k and its fluxes, respectively, their components are values at nodal points of the corresponding boundaries, A and B are square, generally not symmetric matrices of approximations, and quantities with superscript in are assigned to the nodal points at Γ_C and that with the superscript out are connected with the values outside of Γ_C . Since on Γ_C it holds $u_f^{\text{in}} = u_m^{\text{in}}$ and $q_f^{\text{in}} + q_m^{\text{in}} = q_C$, one eventually gets:

$$\begin{bmatrix} K_{11}^f & K_{12}^f & 0 \\ K_{21}^f & K_{22}^f + K_{11}^m & K_{12}^m \\ 0 & K_{21}^m & K_{22}^m \end{bmatrix} \begin{Bmatrix} u_f^{\text{out}} \\ u_f^{\text{in}} \\ u_m^{\text{out}} \end{Bmatrix} = \begin{Bmatrix} q_f^{\text{out}} \\ q_C \\ q_m^{\text{out}} \end{Bmatrix} \quad (21)$$

where the matrix of the system is banded but generally nonsymmetrical. Using the periodic boundary conditions $u_f^{out}=u_m^{out}=0$ due to the symmetry, cf. Suquet (1985) in elasticity, the unknowns q on $\partial\Omega$ follow from the previous equation. Moreover, with respect to Eq. (3),

$$q = c\left(\frac{\partial u_1}{\partial y_i} + \frac{\partial u_0}{\partial x_i}\right) \Rightarrow \langle q \rangle = c^* \langle \nabla u \rangle,$$

where, Lévy (1985):

$$c_{ik}^* = \int_{\Omega} c(y) \left(1 + \frac{\partial w_k}{\partial y_i}\right) d\Omega(y) = c_f \int_{\Omega_f} \left(1 + \frac{\partial w_k}{\partial y_i}\right) d\Omega(y) + c_m \int_{\Omega_m} \left(1 + \frac{\partial w_k}{\partial y_i}\right) d\Omega(y),$$

$$i = 1, 2 \quad (22)$$

Now the advantage of the boundary element formulation appears: applying the Green theorem leads us to interface integrals as:

$$c_{ik}^* = c_f \text{meas } \Omega_f + c_m \text{meas } \Omega_m + c_f \int_{\partial\Omega_f} w_k n_i^f d\Omega(y) + c_m \int_{\partial\Omega_m} w_k n_i^m d\Omega(y) =$$

$$= c_f \text{meas } \Omega_f + c_m \text{meas } \Omega_m + c_f \int_{\partial\Omega_f - \Gamma_C} w_k n_i^f d\Omega(y) + c_m \int_{\partial\Omega_m - \Gamma_C} w_k n_i^m d\Omega(y) +$$

$$+ c_f \int_{\Gamma_C} w_k n_i^f d\Omega(y) + c_m \int_{\Gamma_C} w_k n_i^m d\Omega(y)$$

$$(23)$$

so that the unpleasant volume integrals in (22) is substituted by boundary integrals, and even by the integrals which are separated into external boundary and the interface. Note that $c_{ik}^* = c^*$ because of the axial symmetry considered.

5 Optimization

Similarly to the optimization of beams, Prochazka et al (2009), an energy functional Π is formulated on an admissible set of fiber domains; Lagrangian multiplier constraints the value of the given area of fiber. A natural question for engineers dealing with composites could be as: determine such a shape of the fibers that enable it to decrease the overall conductivity of the entire composite structure and attains its minimum. In the same time a minimum flux is required. This is a problem of optimal shape of structures. Generally, let us have a given domain Ω_f and the temperature field u , which is the solution of an appropriate partial differential equation or, alternatively, it follows from a corresponding variational principle. Obviously, the temperature field is strongly dependent on the domain Ω_f . From

these arguments a formulation of the real functional $\Pi \equiv \Pi(u, \Omega_f)$ should be created. Then the problem of optimal shape consists of finding such a domain $\Omega_f \subset \Omega$ from a class O of admissible domains (to be stated later on), which minimizes with respect to the shape of Ω^f . This may symbolically be written as

$$\min_{u \in \Omega, \Omega^f \in O} \Pi(u, \Omega^f) \tag{24}$$

Since there is no external loading in our solution and the load is due to fluxes on the interfacial boundary Γ_C , one of an appropriate formulations meeting the above requirements is an assumption of minimum strain energy of a structure subject to the above mentioned load distribution. Such a problem may be formulated in terms of minimum Lagrangian. In our case, we assume the constant volume of fibers, i.e. $\text{meas } \Omega^f = v_f$, where v_f is the fiber volume fraction. The extended Lagrangian involving the volume (area) constraint using the Lagrangian multiplier is written as:

$$\begin{aligned} \Pi(u, \Omega_f) &= \frac{1}{2} \int_{\Omega} q \nabla u \, d\Omega(y) - \lambda \left(\int_{\Omega_f} d\Omega - \text{meas } \Omega_f \right) = \\ &= \frac{1}{2} \langle q \rangle \langle \nabla u \rangle - \lambda \left(\int_{\Omega_f} d\Omega - \text{meas } \Omega_f \right) \rightarrow \text{stationary} \end{aligned} \tag{25}$$

It remains to select the design parameters of this optimization problem and the admissible set O of the domains. Let the domain of fiber Ω^f be star-shaped and the pole is centered at the unit cell Ω . Hence, the interfacial boundary describing the shape of the fiber can be defined in polar coordinates as: For any Ω^f there is a function $r : [0, \pi/2] \rightarrow (0, 1)$ such that

$$\Gamma_C \equiv \{(\hat{y}_1(\phi), \hat{y}_2(\phi)); \phi \in [0, \pi/2]\} \tag{26}$$

where

$$\hat{y}_1(\phi) = r(\phi) \cos \phi, \quad \hat{y}_2(\phi) = r(\phi) \sin \phi$$

and certainly only the first quarter is assumed for calculation. The approximation $\bar{\Gamma}_C$ of the interfacial boundary Γ_C is created as follows: the beams originating at the center of the unit cell and ending at selected points of the interfacial boundary Γ_C (nodal points) are described as $r = \{r_1, r_2, \dots, r_n\}$, which identify also the their length, and n is the number of the beams. This is a natural choice describing the current position of the interfacial boundary $\bar{\Gamma}_C$ and its movements assuming the polygonal approximation of the interface. Moreover, the approximation $\bar{\Gamma}_C$ defines

$\bar{\Omega}^f$. Any approximated interfacial boundary $\bar{\Gamma}_C$ will be created by a sequence of abscissas Γ_C^f their end points N_0, N_1, \dots, N_n are identified as:

$$N_i = \{(\bar{y}_1(\phi_i), \bar{y}_2(\phi_i)); \phi_i = \frac{\pi i}{2n}\} \tag{27}$$

so that the division of the angle intervals is uniform. In this case the design parameters p will be identified with the radii $r_i = r(\phi_i)$ connecting N_i with the origin of the coordinate system. Now the appropriate design parameters are recorded in the vector $p \equiv \{p_1, p_2, \dots, p_n\}$, identifying the change of the boundary of fibers Γ_C , which is divided into n nodal points $N_1, N_2, \dots, N_i, \dots, N_n$. These points are connected with the natural origin 0 of the local coordinate system, see Fig. 2. Note that in the sequel the primes identifying the approximations of the fiber domain are omitted, for simplicity.

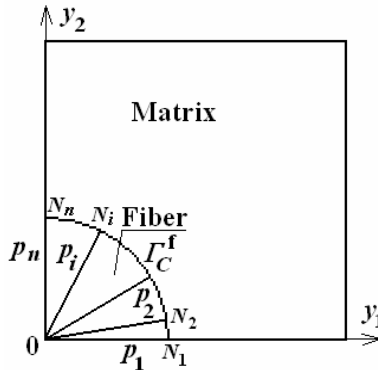


Figure 2: Description of design parameters

Moreover, from a practical experience is necessary to add additional constraints to keep the problem in realistic limits. On one hand side the requirements are impacts of the numerical method used (too close Γ_C to $\partial\Omega$ is not desired), i.e. $\text{dist}\{\Gamma, \Gamma_C\} \geq d > 0$, where dist is the minimum distance between points at Γ and Γ_C , on the other hand there may not be any crossing of $\partial\Omega$ and Γ_C , i.e. $\partial\Omega \cap \Gamma_C = \emptyset$. The points at Γ_C cannot be too close to the origin of the coordinate system. The above mentioned conditions could be summed up as:

1) $p_i \geq a, i = 1, \dots, n$ (the lower bound has meaning that no nodal point of the interfacial boundary between the fiber and matrix can be too close to the singular point centered at the origin of local coordinates); note that in our numerical experiments we select $a = 0.1 \text{ mm}$

2) $p_i/\sin \phi_i \leq d$, $p_i/\cos \phi_i \leq d$, $i = 1, \dots, n$ (the upper bound means that the nodal points of the interface cannot be too close to the external boundary of the unit cell), in our numerical experiments we select $d = 0.1$ mm

In view of the above arguments the admissible set O is defined by:

$$O \equiv \{\Omega^f \subset \Omega; \text{ it is star shaped and obeys the above conditions 1) and 2)} \quad (28)$$

In this way one obtains n triangles T_s , $s=1, \dots, n$, which approximate the domain Ω_f . It obviously holds:

$$\int_{\Omega^f} d\Omega = \text{meas } \Omega_f = \sum_{s=1}^n \text{meas } T_s. \quad (29)$$

If the above bounds on the beams are attained a special procedure needs to be used, see Suquet (1985). It requires an internal iteration, in order to improve the boundary using collinear mapping for ensuring the condition about constant fiber volume fraction.

It is worth noting that other constraint conditions can be applied, see e.g. Suquet (1985).

5.1 Euler's equations

The stationary requirement leads to differentiation of the functional by the shape (design) parameters

$$\lambda = P_s \frac{\frac{1}{2} \langle \nabla u \rangle \frac{\partial c^*}{\partial p_s} \langle \nabla u \rangle}{\frac{\partial}{\partial p_s} \int_{\Omega^f} d\Omega}, \quad s = 1, \dots, n \quad (30)$$

Equation (30) requires λ having the same value for any s . In other words, if this requirement were attained at any point on the "moving" part of the interfacial boundary the optimal shape of the trial body would be reached. For this reason the body of the composite structure should increase its area (in 3D its volume) at the nodal point of the boundary identified by p_s if λ is larger than the true value of the target, while it should decrease its value when λ is smaller than the correct Lagrangian multiplier. As, most probably, real value of the target is not known a priori, its estimate is done by averaging the current values at the nodal points. So, approximation of λ will be expressed as:

$$\lambda_{\text{approx}} = \frac{1}{n} \sum_{s=1}^n \lambda_s \quad (31)$$

Differentiation by λ completes the system of Euler's equations by Eq. (26).

It remains to ensure that the fiber volume friction is constant with the value given a priori. For this aim a collinear mapping is applied after completing the shift of nodes at the interface. It can be done in such a way that assuming the current value of $\text{meas } \Omega_{\text{curr}}^f$, which is calculated from the current positions of the nodes mentioned, the prescribed $\text{meas } \Omega^f$ is reached by improving the triangles by the value of

$$s = \sqrt{\frac{\text{meas } \Omega_{\text{curr}}^f}{\text{meas } \Omega^f}} \tag{32}$$

The idea of calculating a general area bounded by a polygonal boundary is seen from Fig. 3. The pole P is one vertex of a current triangle and the nodes on the boundary are another two. Since the identification of the vertices is obvious from their coordinates, a well known formula is applicable for calculating the influence of the current triangle to the area. Positive triangles are located on the boundary which is farther from the pole and they add their values to the area while the negative triangles are on the boundary which is closer to the pole.

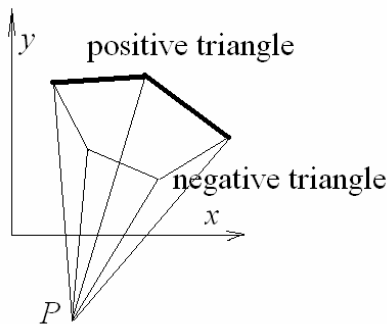


Figure 3: Calculation of the area of domain

Brief description of algorithm:

1. set up the starting configuration fulfilling the condition given by Eq. (26)
2. calculate c^* for the current configuration
3. set a successive unit shifts to nodal points p_s at Γ_c , calculate $c^*(p_s)$, and the appropriate λ from Eq. (30) using substitution of derivatives by differences (central difference is used here and the step of difference is 0.0001)

4. compute λ_{approx} by Eq. (31) to get new positions of nodes at
5. from the new positions get the area of the current Ω_f
6. using collinear mapping (32) improve the positions of nodes to ensure the original fiber volume ratio
7. check up the constraint of the beams p_s and if fail occurs apply local iteration
8. the process of iterations end if the absolute value of difference between current and previous energies λ_{approx} be less then given admissible error; if not, go to 2 and stop otherwise

6 Numerical examples

Unit cell is considered with various fibers volume ratios. Since we compare energy densities at nodal points of the interfacial boundary, the relative energy density may be regarded as the comparative quantity influencing the movement of the boundary Γ_c . As said in the previous section, the higher value of this energy density, the larger movement of the nodal point of should aim at the optimum.

In the following examples minimum conductivity u is required, and the fiber v_f and matrix v_c phase ratios and the values of fiber c_f and matrix c_m conductivities are also given.

The problem is solved, as said previously, on the first quarter (0.5×0.5) of the axially symmetric unit cell. The distribution of interfacial nodal points obeys a rule that they are positioned at beams with the beginning at the origin. The adjacent beams are rotated by the same angle. In the sequel 17 nodal points in the interface (excluding the external boundary) are used in every example.

The boundary element mesh is shown for a typical example $v_f = 0.5$, $v_m = 0.5$ in the initial geometry in Fig. 4., and in Fig. 5 at the optimal stage. The nodal points change as a spider web.

In the first numerical test $c_f = 5$ and $c_m = 1$. In Figs. 6 to 9 the optimal shapes are shown for various phase volume fractions. The phase with higher conductivity is darker then that with lower value. In the following pictures the darker area points out the phase possessing the higher conductivity.

In Fig. 6 an additional constraint $a = 0.05$ has been applied, as the too small fiber causes too small distance to the origin. The optimal shape in Fig. 7 does not desire any additional condition. In Fig. 8 and Fig. 9 there are constraints given by $d = 0.45$.

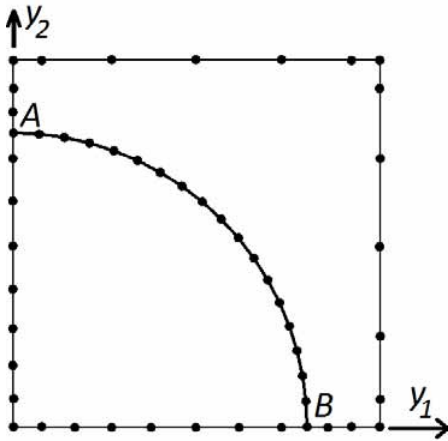


Figure 4: Initial geometry

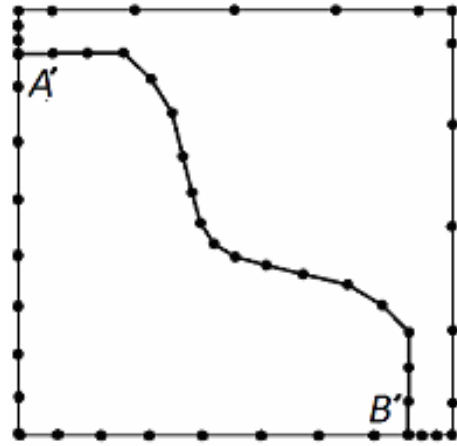
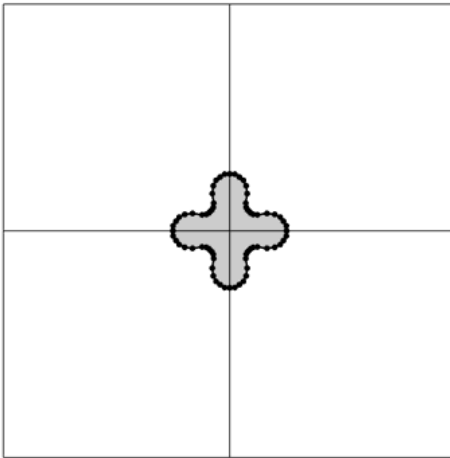
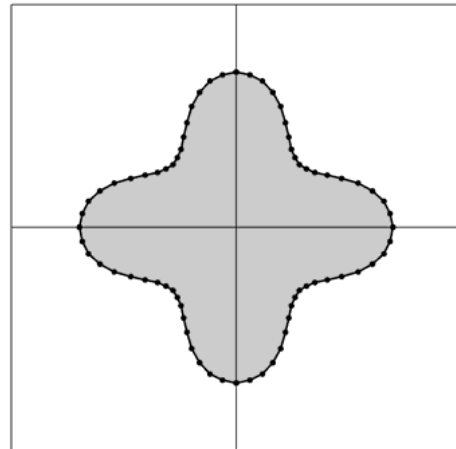


Figure 5: Nodes at optimal shape

Figure 6: $c_f = 5$, $c_m = 1$, $v_f = 0.05$, $v_m = 0.95$ Figure 7: $c_f = 5$, $c_m = 1$, $v_f = 0.25$, $v_m = 0.75$

In the next examples fiber possesses lower conductivity of $c_f = 1$ then the matrix, which has $c_m = 5$. Figs. 10-12 show the optimal shapes for various fiber volume fractions.

In Fig. 13 a typical course of error vs. iteration together with percentage time consumption are demonstrated. The error drops very quickly and, say, from 15-th iteration is almost no deviation from the optimal shape. The picture is depicted for

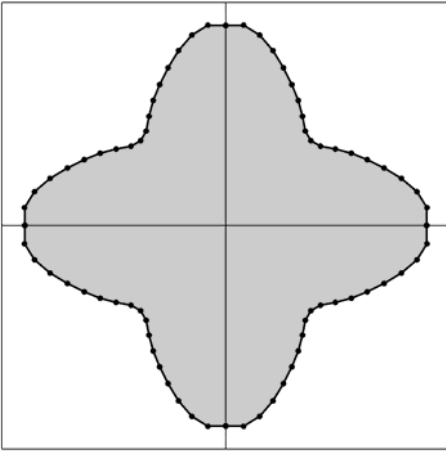


Figure 8: $c_f = 5$, $c_m = 1$, $v_f = 0.05$, $v_m = 0.95$

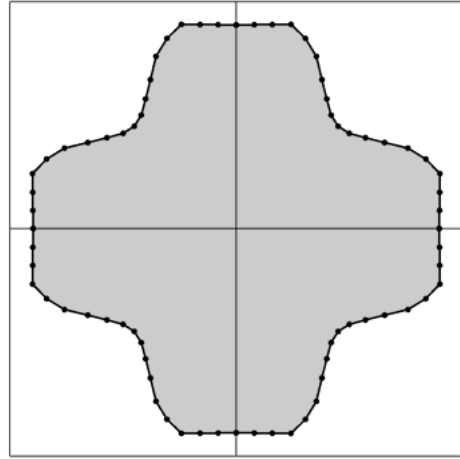


Figure 9: $c_f = 5$, $c_m = 1$, $v_f = 0.25$, $v_m = 0.75$

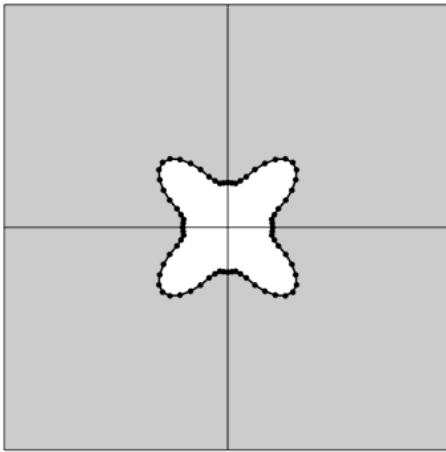


Figure 10: $c_f = 1$, $c_m = 5$, $v_f = 0.05$, $v_m = 0.95$

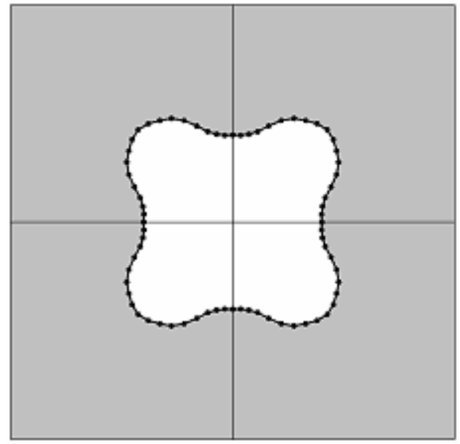


Figure 11: $c_f = 1$, $c_m = 5$, $v_f = 0.2$, $v_m = 0.8$

the case displayed in Fig. 9, i.e., additional calculations have to be conducted in this case due to the violation of the limits imposed to admissible beams. After attaining at the limit state of at least one beam the iteration causes delay in time consumption. This is caused by an “internal iteration”, which assures the fulfillment of the admissibility of the length of any beam in the selected set of design parameters.

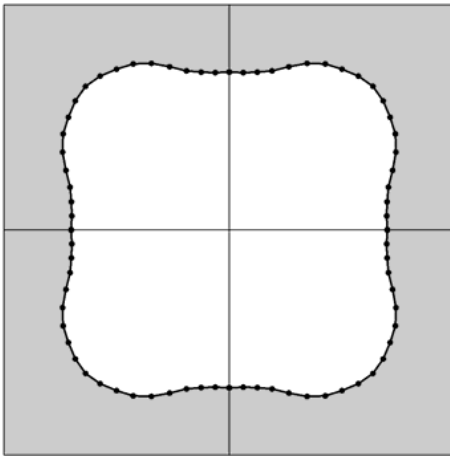


Figure 12: $c_f = 1$, $c_m = 5$, $\nu_f = 0.5$, $\nu_m = 0.5$

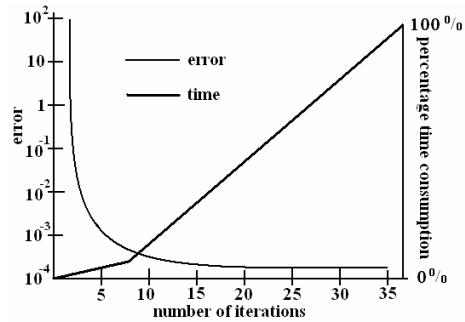


Figure 13: typical error and time curve

7 Conclusions

New optimization procedure is put forward in this paper based on homogenization technique. The problem which has been solved deals with homogenization of coefficients of the linear harmonic equation. The optimization is formulated in term of energy. A special constraint is adopted, which is involved in the formulation of optimal shape by Lagrangian multiplier, enabling us to show that the stationary point is attained for energy density being equal at each nodal point of the interfacial boundary. This condition leads us to an elegant and efficient numerical approach. The computer program now enables the user to get various optimal shapes according to his requirements.

Two basic material properties of phases have been adopted. In the first option a higher conductivity in fiber is adopted and then a higher conductivity in matrix is considered. From these experiments it appears that in both cases curvilinear shape is desired, in one case the longest beams heads in the coordinate direction and in the second in the direction of the main axis of the first quarter. In every case a shape of a star with four vertices is desired to get the optimum.

Acknowledgement: Financial support of the Grant agency of the Czech Republic, grant number P105/00/0266 is gratefully acknowledged.

References

- Akad, Z.K.; Aravinthan, T.; Yan Zhub, Y.; Gonzalez, F.** (2012): A review of optimization techniques used in the design of fibre composite structures for civil engineering applications. *Materials and Design*, 33, pp. 534–544.
- Allaire, G.** (2001): Shape Optimization by the Homogenization Method, Applied Mathematical Sciences – Volume 146. *Shape optimization by the homogenization method*. Springer, pp. 456.
- Challis, V.J.; Roberts, A.P.; Wilkins, A.H.** (2008): Design of three dimensional isotropic microstructures for maximized stiffness and conductivity. *Int. J. Solids and Structures*, 45, (14-15), pp. 4130-4146.
- Dvorak, J.** (1996): *Optimization of composite materials*, Ph.D. thesis, Charles University, June.
- Haslinger, J.; Dvorak, J.** (1995): Optimum composite material design. *RAIRO*, 29(6), pp. 657-686.
- Lévy, T.** (1985): Fluids in porous media and suspensions. *Lecture Notes in Physics* 272 (eds. E. Sanches-Palencia and A. Zaoi) Part II, Springer Verlag Berlin, pp. 64-119.
- Prochazka, P.P.; Dolezel, V.; Lok, T.S.** (2009): Optimal shape design for minimum Lagrangian. *Eng. Anal. with Bound. Elem.*, 33, pp. 447–455.
- Prochazka, P.P.** (2012a): Fiber shape optimization in linear elasticity. *BETEQ* Prague, September, pp. 61-66.
- Prochazka, P.P.** (2012b): BEM shape optimization of a hole in composite for minimum Lagrangian. 18th International Conference *Engineering Mechanics*, pp. 1073–1080.
- Suquet, P.M.** (1985): Homogenization techniques for composite media. *Lecture Notes in Physics* 272 (eds. E. Sanches-Palencia and A. Zaoi) Part IV, Springer Verlag Berlin, pp. 194-278.
- Zhou, S.; Lia, Q.** (2008): Computational Design of microstructural Composites with tailored thermal conductivity. Numerical Heat Transfer, Part A: Applications. *Int. J. Comp. and Methodology*, 54(7), pp. 686-708.

